

Crystalline Xenon—A Kinematic Low-Energy Electron-Diffraction Spectrum*

A. Ignatjevs, J. B. Pendry,[†] and T. N. Rhodin

Department of Applied Physics, Clark Hall, Cornell University, Ithaca, New York 14850

(Received 5 October 1970)

Intensity-energy low-energy electron-diffraction spectra of a clean xenon single-crystal surface have been measured for the first time, and show almost no secondary structure. A theoretical explanation is given based on the large atomic volume of xenon, and the short extinction distance (of about 5 Å) at 100 eV.

In measuring the intensities of electrons elastically scattered from crystal surfaces many more peaks are seen than can be explained by simple Bragg reflection. Calculations for strong-scattering atoms¹⁻⁸ show that the additional structure can be caused by multiple scattering. Realistic calculations of the atomic potential^{3,8} and inelastic scattering⁹ show that part of the elastic scattering (that which occurs in the forward direction) is of the same order as, or larger than, the inelastic scattering, and hence the electron is forward scattered several times before it is removed by inelastic scattering, or backscattered out of the crystal.⁵ Whereas this course of events can be accounted for by several current theories,^{5,8} all these theories require as input several parameters for the crystal and its surface, e.g., the scattering potential. Further the theories are nonlinear in these parameters which makes direct inversion of the problem impossible. One can only proceed by successively refining guesses: a difficult process with the number of parameters essential to a calculation of a low-energy electron-diffraction (LEED) spectrum (there are, for example, at least four or five phase shifts required to give an accurate picture of the elastic potential alone). On the other hand, if it were possible to find a material whose spectrum is adequately described by kinematic theory, the reflected amplitudes would become linearly dependent on many of the parameters, and

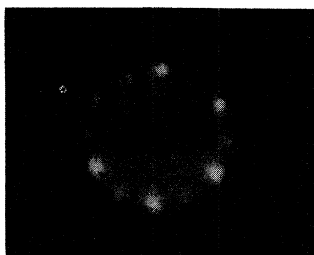


FIG. 1. LEED pattern from crystalline xenon, (111) surface, at 83.5-V incident energy and 40°K. It shows the four-domain structure obtained by growing xenon on a clean iridium (100) surface.

inversion becomes a simple process. We claim to have found just such a system in xenon single-crystal films at low temperatures.

Several authors have reported studies relevant to the growth and structure of inert gas crystals deposited on substrates.¹⁰⁻¹⁴ In this study well-defined LEED patterns were obtained from thick epitaxial xenon single-crystal films (Fig. 1) and for the first time, reproducible intensity-energy spectra and Auger spectra were measured. Experimental details indicating the conditions under which well-ordered contamination-free crystals were produced, and surface composition monitored by Auger spectroscopy, are reported elsewhere.¹⁵ An intensity-energy curve taken from a xenon crystal grown on a clean well-ordered iridium (100) surface is shown in Fig. 2. The angle of incidence is 5.5° away from normal incidence, and the temperature is 40°K. Above 25 eV (a) the peaks have a simple Lorentzian shape, (b) there is one and only one peak for every Bragg reflection expected, (c) deviation from the Bragg positions after correction for a constant inner potential is very small, less than a

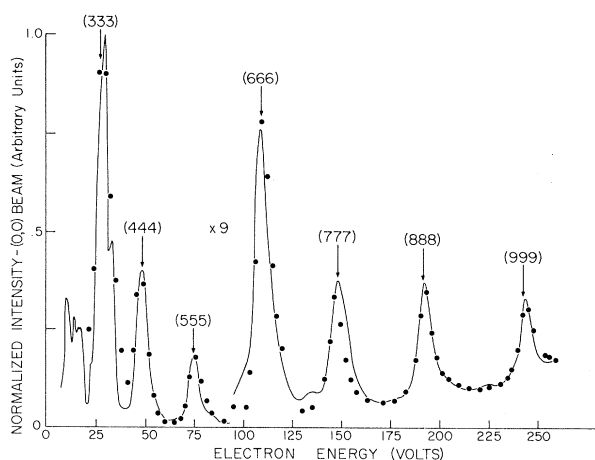


FIG. 2. Normalized intensity-energy curve for crystalline xenon taken at 5.5° away from normal incidence, the temperature being 40°K. Dots show the result of a kinematic calculation using a constant inner potential of 10.0 eV.

volt, (d) secondary structure is discernable, but only just, and (e) spectra taken at greater angles of incidence show no tendency for the peaks to split. Thus, above 25 eV all the usual conditions by which we identify kinematic scattering are satisfied. Below 25 eV secondary structure becomes stronger as inelastic scattering gets weaker.

We can explain how this comes about, in the following manner. Kinematic theory is retrieved when the matrix elements for inelastic scattering, V_i , are much larger than the largest elastic-scattering matrix elements V_f . In nickel the experimentally observed nonkinematic scattering¹⁶ implies that this condition is not satisfied. This is borne out by Pendry's calculation^{3,4} of V_f and extraction from experiment⁵ of V_i :

$$V_f = -5 \text{ to } -10 \text{ eV}, \quad (1)$$

$$V_i \approx -3 \text{ eV}. \quad (2)$$

In the case of xenon we obtain V_i in the following way. A general theory⁵ has been derived, covering both multiple scattering and kinematic situations, relating widths of peaks in intensity-energy spectra, ΔE , to V_i :

$$\Delta E = 2V_i. \quad (3)$$

From Fig. 2 we deduce that $V_i \sim 4$ eV for xenon over a wide range of energies. Now let us consider the elastic scattering. It is widely known that scattering factors, apart from resonances, do not vary from atom to atom by more than a factor of 2, or thereabouts. The cancellation theorem^{17,18} tells us why this should be so: The core region of the atom contributes only multiples of π to the phase shift, which do not affect the scattering. By way of example we cite the cases of gold¹⁹ and copper,²⁰ two materials with similar scattering factors and hence similar properties, but with very different atomic numbers. However, the scattering factor has to be divided by the atomic volume to give the matrix elements. The heavier rare gases are distinguished by large atomic volumes. The atomic volume of xenon is 60 \AA^3 , or about eight times that of nickel! Assuming elastic scattering factors of the same order of magnitude for nickel and xenon, we retrieve for xenon

$$V_f \approx -1 \text{ to } -2 \text{ eV}, \quad (4)$$

$$V_i \approx -3.5 \text{ to } -4.5 \text{ eV}. \quad (5)$$

The inequality required for kinematic scattering is now satisfied for xenon, and secondary structure should be less intense than primary

structure by a factor of $(\frac{1}{4})^2$, which is approximately the case. In addition, below 25 eV where peak widths imply that V_i is ~ 1 eV, we begin to observe secondary structure increase in size, consistent with our estimates of V_f . Thus, the highly polarizable outer shell of xenon apparently keeps inelastic scattering large, but at the same time the huge size of the atomic volume reduces the effect of elastic scattering. One might expect to see similar effects in some of the other inert gases that also have large atomic volumes.

Finally, we illustrate our point about inversion of experimental data in the kinematic case. A plot of the energies of those peaks above 25 eV against the square of their order yields a lattice spacing of 6.16 \AA compared with the x-ray figure²¹ at 40°K of 6.154 \AA , and an inner potential of 10.0 eV. The positions of the Bragg peaks consistent with these data are shown by vertical lines in Fig. 2. Using the peak widths to obtain V_i and the heights to obtain $|T|^2$ (the scattering factor, which automatically includes the Debye-Waller factor) and inserting these numbers into a kinematic calculation of reflected intensities gives results which have been plotted as dots in Fig. 2.

We have observed an interesting effect which occurs in the seventh-order peak at 148 eV. This peak is much weaker than the sixth-order one, and of about the same intensity as the eighth-order peak, despite the rapidly increasing Debye-Waller factor. We believe that this is due to $|T|^2$ having one of the steep minima that is often seen in calculated scattering factors,²² at this particular angle and energy. Hence, second-order processes have greater relative importance, and it is the secondary peaks appearing as shoulders on the main Bragg peak that appear to increase the width. Additional evidence is given by the fact that $1\frac{1}{2}^\circ$ farther away from normal incidence the seventh-order peak increases rapidly in intensity by a factor of 2, and becomes more narrow, in conformity with the widths of its neighbors (Fig. 3).

Clearly curves which are so readily amenable to theoretical interpretation greatly extend the scope of the information one can extract from LEED spectra. In the near future it is hoped to report on several experiments. Among these there will be a determination of Debye temperatures in an almost kinematic system, in which the electrons are much more localized near the surface layers than in other materials (at 30 eV about 70% of the wave function of an electron scattering from xenon lies within the first layer

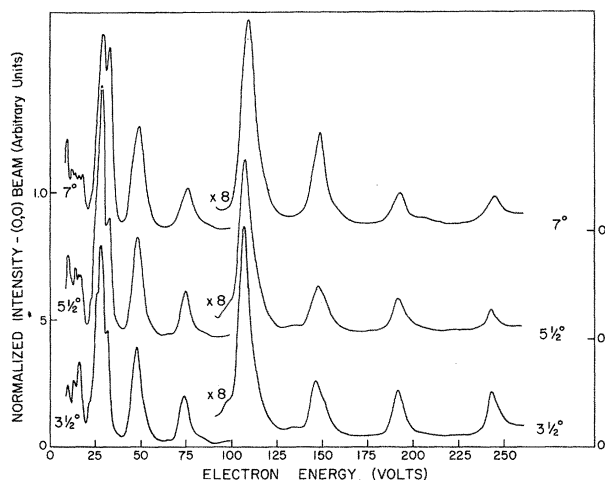


FIG. 3. Normalized intensity-energy spectra for crystalline xenon taken at 3.5°, 5.5°, and 7° away from normal incidence at 40°K, showing the general trend with angle of incidence. The relative attenuation of the seventh-order Bragg peak for the 5.5° curve is significant (see text).

of atoms), and the experimental determination of the modulus of the atomic scattering factor for a range of angles and energies.

The preliminary work in this study, particularly the LEED observation of xenon crystal epitaxy, by Dr. Arthur V. Jones is gratefully acknowledged. Research support from the U. S. Air Force Office of Scientific Research and from the Advanced Research Project Agency through the Cornell Materials Science Center is also gratefully acknowledged.

*Work supported by U. S. Air Force Office of Scientific Research Grant No. 68-1586.

†Visiting scientist. Permanent address: The Caven-

dish Laboratory, Cambridge, England.

¹E. G. McRae, *J. Chem. Phys.* **45**, 3258 (1966).

²P. M. Marcus and D. W. Jepsen, *Phys. Rev. Lett.* **20**, 925 (1968).

³J. B. Pendry, *J. Phys. C: Proc. Phys. Soc., London* **2**, 1215 (1969).

⁴J. B. Pendry, *J. Phys. C: Proc. Phys. Soc., London* **2**, 2273 (1969).

⁵J. B. Pendry, *J. Phys. C: Proc. Phys. Soc., London* **2**, 2283 (1969).

⁶C. B. Duke and C. W. Tucker, Jr., *Phys. Rev. Lett.* **23**, 1163 (1969).

⁷C. B. Duke and C. W. Tucker, Jr., *Surface Sci.* **15**, 231 (1969).

⁸J. A. Strozier, Jr., and R. O. Jones, *Phys. Rev. Lett.* **25**, 516 (1970).

⁹B. I. Lundqvist, *Phys. Status Solidi* **32**, 273 (1969).

¹⁰J. J. Lander and J. Morrison, *Surface Sci.* **6**, 1 (1967).

¹¹R. F. Steiger, J. M. Morabito, Jr., G. A. Somorjai, and R. H. Muller, *Surface Sci.* **14**, 279 (1969). See also L. A. Bruce, *Surface Sci.* **20**, 183 (1970); R. F. Steiger, J. M. Morabito, Jr., G. A. Somorjai, and R. H. Muller, *Surface Sci.* **20**, 190 (1970).

¹²P. W. Palmberg, in *30th Annual Conference on Physical Electronics*, Milwaukee, Wis., 30 March 1970 (to be published).

¹³J. M. Dickey, H. H. Farrell, and M. Strongin, *Surface Sci.* **23**, 448 (1970).

¹⁴D. J. Ball and J. A. Venables, *J. Vac. Sci. Technol.* **6**, 468 (1969).

¹⁵A. Ignatjevs, A. V. Jones, and T. N. Rhodin, to be published.

¹⁶L. G. Feinstein, *Surface Sci.* **19**, 366 (1970); R. L. Park and H. E. Farnsworth, *Surface Sci.* **2**, 527 (1964).

¹⁷M. H. Cohen and V. Heine, *Phys. Rev.* **122**, 1821 (1961).

¹⁸J. B. Pendry, to be published.

¹⁹H. Schlosser, *Phys. Rev.* **131**, 491 (1970).

²⁰G. A. Burdick, *Phys. Rev.* **129**, 138 (1963).

²¹G. L. Pollak, *Rev. Mod. Phys.* **36**, 748 (1964).

²²J. B. Pendry, to be published.

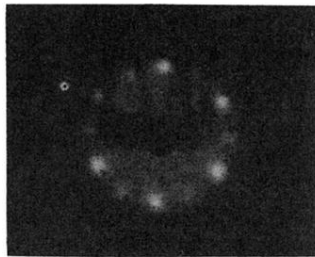


FIG. 1. LEED pattern from crystalline xenon, (111) surface, at 83.5-V incident energy and 40°K. It shows the four-domain structure obtained by growing xenon on a clean iridium (100) surface.